




Research Article

Optimization of FDM Printing Process Parameters on Surface Finish, Thickness, and Outer Dimension with ABS Polymer Specimens Using Taguchi Orthogonal Array and Genetic Algorithms

Jasgurpreet Singh Chohan ¹, Raman Kumar ¹, Aniket Yadav,¹ Piyush Chauhan,¹ Sandeep Singh ², Shubham Sharma ^{1,3}, Changhe Li,⁴ Shashi Prakash Dwivedi,⁵ and S. Rajkumar ⁶

¹Department of Mechanical Engineering, Chandigarh University, Mohali 140413, India

²Department of Civil Engineering, Chandigarh University, Mohali 140413, India

³Deptt. of Mechanical Engg., IK Gujral Punjab Technical University, Main Campus, Kapurthala 144603, India

⁴School of Mechanical and Automotive Engineering, Qingdao University of Technology, Qingdao, 266520, China

⁵G.L. Bajaj Institute of Technology & Management, Greater Noida, Gautam Buddha Nagar, UP 201310, India

⁶Department of Mechanical Engineering, Faculty of Manufacturing, Institute of Technology, Hawassa University, Awasa, Ethiopia

Correspondence should be addressed to Shubham Sharma; shubhamsharmacsircrli@gmail.com and S. Rajkumar; ccetraj@gmail.com

Received 7 November 2021; Revised 13 January 2022; Accepted 31 January 2022; Published 11 March 2022

Academic Editor: Jiafu Su

Copyright © 2022 Jasgurpreet Singh Chohan et al. This is an open access article distributed under the Creative Commons Attribution License, which permits unrestricted use, distribution, and reproduction in any medium, provided the original work is properly cited.

Fused deposition modelling (FDM) is a technique of additive manufacturing used to fabricate a 3D (three-dimensional) model with layer-by-layer deposition of required materials with less material wastage. FDM is used to make any objects with a meager cost, but also there are some negative points related to less strength, less accuracy, and less surface finish. In this study, acrylonitrile butadiene styrene (ABS) is printed using an FDM printer to investigate the effects of various changing parameters like nozzle temperature (°C), infill pattern, and printing speed (mm/s) on surface roughness and thickness measurement. Experiments are designed using the Taguchi L9 orthogonal array method and ANOVA method. For obtaining an increase in surface roughness, the most influencing factor is printing speed with 83.41% contribution, and the effect of nozzle temperature is 9.04%. Lesser printing speed enhances the surface finish and, in the case of thickness and outer dimension of all the printed samples, results are almost constant. Regression analysis is performed to formulate the single-objective equations, and a genetic algorithm (GA) is applied to optimize the values of process parameters.

1. Introduction

Additive manufacturing is a rapidly growing technique that has significant advantages over conventional subtractive manufacturing techniques. In this technique, design is prepared in CAD software and printed layer by layer using three-dimensional (3D) printers and a final 3D solid is obtained [1]. It is also used to make joint fewer products or

specimens comparatively higher the strength than the material removal process [2]. Additive manufacturing is used to make complex structures like dental implants [3], hip implants [4], gears [5], and many other objects which are difficult to manufacture by using subtractive manufacturing techniques. It is used in almost every field of application like biomedical industry [6], aerospace industry [7], automotive industry [8], food printing [9], and teaching [10] also. These

3D printers can be of different types and are based up different principle techniques [11]. Different printers have different states of input material like powder form and filament form. 3D printers can be of many types like SLA [12], SLS [13], LOM [14], and FDM [15], which are commonly used in industry. FDM is most widely used due to its easy construction, low cost, and maintenance [16]. In FDM, the parts having complex geometries are rapidly created through numeric controlled nozzles through layer-by-layer manufacturing while no clamps, jigs, and fixtures are required as traditional manufacturing processes. The FDM incorporates a desktop prototyping facility in the office as it uses nontoxic, odourless, and environmentally friendly materials. Due to the good chemical and mechanical properties, the FDM parts are highly suitable for conceptual modelling, functional prototypes, and end-use production parts. The demand of tight dimensional tolerances and complex design features that were unobtainable with traditional processes became practical with FDM technology. Consequently, AM technology has been adopted by various biomedical, automotive, aerospace, and electronics industries.

In fused deposition modelling, the parts are digitally manufactured layer by layer extruding a small bead of heated plastic material (0.5°C above melting point) by robotically controlled nozzle head moving in X and Y directions on a fixtureless table. After one layer is deposited, the extrusion nozzle head is numerically raised relative to the table to deposit subsequent layers of the part. Similar to other AM processes, the FDM also requires support structures to be added beneath the overhanging features, which are later removed. Support material is extruded through other nozzle acting as scaffolding which is water soluble and afterward removed from the substrate. As FDM is evolving with enormous pace today, it can be used for printing of various materials like polymers [17], composites [18], biomaterials [19], wood [20], food materials [9], and ceramics [21]. Out of all these materials, polymers are widely used. PLA and ABS are two widely used polymers due to several unique advantages like both are thermoplastics (can be reused), and both can be made into the filament form and hence can be used in FDM printers [22]. The present study has focused on the impact of FDM process parameters on surface roughness and dimensional accuracy. Furthermore, multiresponse optimization has been performed to identify an optimum set of parameters for both responses.

The rest of the paper is organized as follows: Section 2 presents the relevant literature. Section 3 provides the details of the experimental setup. Section 4 presents the optimization of process parameters. The last section provides the concluding remarks.

2. Literature Review

FDM is an additive manufacturing technique that depends upon various printing parameters. Ali et al. (2019) have predicted the dynamic mechanical properties of the printed structure. Various parameters like raster angle, air gap, and build orientation were changed for the evaluation purpose

and, according to this design, artificial neural network (ANN) model was developed and the accuracy is increased within 5% [23]. Wankhede et al. [24] have investigated the surface roughness with changes in parameters like build time on bed, infill density, and layer thickness. Taguchi L9 method is applied to optimize the process and found that layer thickness was the most influencing parameter. Chohan et al. [25] used the Taguchi and ANOVA for 3D-printed parts using FDM and vapour smoothing. In this experiment, six parameters were taken and derived using the Buckingham Pi theorem; it was also found that after a number of cycles of vapour smoothing, there is an increase in the percentage of surface finish. Wang et al. [26] established the 3D printing heat-resistant model using resin and nozzle temperature, printing speed, and layer thickness as the changing parameters. In this work, several structures were made with and without resin, and a surface roughness test was performed. It is found that this model provides a better surface finish. Peng and Yan [27] considered surface roughness and energy consumption simultaneously. After controlling the changing parameters like infill ratio, printing speed, key process parameters, and layers thickness, defined structures were fabricated on three different printers. From this research, it is found that layer thickness was the most influencing parameter for a better surface finish. Yadav et al. [28] have used the ABS and multimaterial in which 60% is ABS and 40% is PETG. Various changing parameters like nozzle temperature, layer thickness, and infill density were taken. In this research work, thirty experiments were performed on Universal Testing Machine and a tensile test was performed. It is found that the specimen with 0.1 mm layer thickness and 225°C nozzle temperature had high tensile strength. Khan et al. [29] used nickel as a coating material due to its lower cost and aesthetic look, and various parameters like raster angle, air gap, and time to metal implant were taken under the maintained environment. It is found from the experiments that there was an increase in the surface of each part. Sajan et al. [30] investigated the circularity and surface roughness of the FDM build part with various changing parameters like bed temperature, nozzle temperature, infill density, print speed, layer thickness, and the number of loops. In this research work, a shape of a grinder blade having some holes is used. It is found that, at the XY plane on the hole, the circularity and surface finish are minimum, while they are maximum at the XZ plane. Ehsanul Haque et al. [31] used the face centered central composite design (FCCCD) as a design of experiments (DOE) to minimize the number of experiments. In this experiment, various changing parameters like layer thickness, raster width, overlap distance, and part orientation were used to design the specimens and to check the surface roughness. It is found that layer thickness was the most influencing parameter to improve the surface finish.

Farina et al. [32] investigated the hardness and bending strength of cement-matrix composites with fractal geometry manufactured through 3D printing. It was found that reinforcements with fractal geometry improved the first crack strength along with residual loading. The interlocking at matrix and ribs of reinforcements delayed the cracking after

the load is exerted. Hibbert et al. [33] evaluated the impact of FDM process parameters on tensile strength through a fully factorial experimental design. It was noted that smaller layer thickness and 90° orientation angle yielded higher mechanical strength. Furthermore, it was found that raster angle has a significant impact on the modulus of toughness, whereas infill pattern influences the yield strength. In a recent study [34], the compressive strength of different 3D-printed materials has been tested. The comparative study has been carried out using PLA, PEEK, ABS, and FDM at different orientation angles. Scanning electron microscope tests reveal that interlaminar pores generated during printing have a significant impact on compressive strength. Furthermore, the compressive strength of different materials also depends upon orientation angle settings. Wang et al. [35] investigated the anisotropic behavior and its impact on the tensile properties of 3D-printed material. The anisotropy increases with a decrease in the strain rate. Also, the tensile fracture observed in a vertical plane is more uniform as compared to a parallel plane.

3. Materials and Methods

In this research work, a total of nine structures were fabricated to investigate the effect of important parameters of important machine parameters like nozzle temperature (°C), infill pattern, and printing speed (mm/s) on the surface roughness. Layer thickness is 0.1 mm, and it is kept constant for all the structures. The schematic diagram of layer deposition is shown in Figure 1. The printing material used for the present investigation is ABS to highlight its wide range of applications.

3.1. Taguchi Procedure for Experimental Design and Analysis. Table 1 shows various parameters designed for the experiment using Taguchi L9 orthogonal array method for optimization. The surface roughness with surface roughness tester and thickness and outer dimension of the gear was measured with the help of a vernier caliper.

3.2. Part Fabrication. The surface roughness, thickness measurement, and outer diameter measurement of ABS with a 3D printer (Prusa i3 Mk2) are investigated. Dimensions of the specimens are 32.9 × 33 × 6 mm with the flat surface only. The infill parameters are infill pattern (lines, triangles, and tetrahedral), nozzle temperature (210°C, 230°C, and 250°C), and layer thickness (60 mm/s, 70 mm/s, and 80 mm/s). Printed specimens are in a shape of a gear, as shown in Figure 2. For the manufacturing of these parts, ABS L400 was used.

4. Results and Discussion

Every 3D-printed part of ABS using the FDM process was measured by time (TR110) surface roughness tester ranging from 0.05– to 10.0 μm, and these printed parts are measured

thrice for better accuracy and after that mean of the readings was taken, as shown in Table 2.

Slow printing speed leads to better surface finish as more time is incorporated for fused material flow and deposition; as ABS is an amorphous type of thermoplastic material, it does not show any true melting point and depicts best printing results near 230°C. Line-type infill pattern shows more surface finish value due to the fact that more area is covered in a line-type pattern as compared to triangular and tetrahedral infill patterns. The effect of various parameters on the surface finish is shown in Figure 3.

Table 3 readings are calculated through the ANOVA method, and printing speed is the most influencing factor here with a percentage of 83.41%. Slow printing speed leads to a better surface finish. Also, the variation due to the nozzle temperature cannot be neglected as it gives 9.04% variation, as shown in Table 3.

4.1. Thickness Measurement of the Structures. The thickness of the 3D-printed part is measured by the analog vernier caliper of Hauser Germany whose least count is 0.02. Readings of each structure were taken thrice for more accuracy. Also, there is little variation in the actual height and observed height or thickness of the specimen, as shown in Table 4 and Figure 4.

The readings in Table 4 show that there is no major effect of variable parameters on the thickness. The thickness of each structure is almost the same, but there is a minor change in value. It can be because of the gum which is applied on the bed due to the poor sticking of ABS.

Readings in Table 5 are calculated through the ANOVA method, and printing speed and infill pattern are the most influencing factors here with a percentage of 46.35% and 39.07%.

4.2. Measurement of the Outer Diameter of the Structures. The outer diameter of the structures was measured by the same above-mentioned vernier caliper. There can be also some change in dimensions as the accuracy of the FDM is less. To take the reading, vernier caliper is placed at the corner of the teeth of the gear and these readings were taken thrice for each structure, as mentioned in Table 6 and Figure 5.

From the above values of the outer diameter of the structure, all the values are almost constant, so there is no major effect of variable parameters like printing speed, nozzle temperature, and infill pattern on the outer diameter. According to the CAD, the design value is 32.9 and the actual value is almost near to 32.70; this small deflection can occur due to less accuracy of FDM-based printers. Table 4 shows the results of thickness measurement.

Readings in Table 7 are observed through the ANOVA method, and here printing speed is the most influencing factor with 87.61% and also the nozzle temperature gives good contribution in the better accuracy with 11.22%. Less printing speed leads to better accuracy, as shown in Table 7.

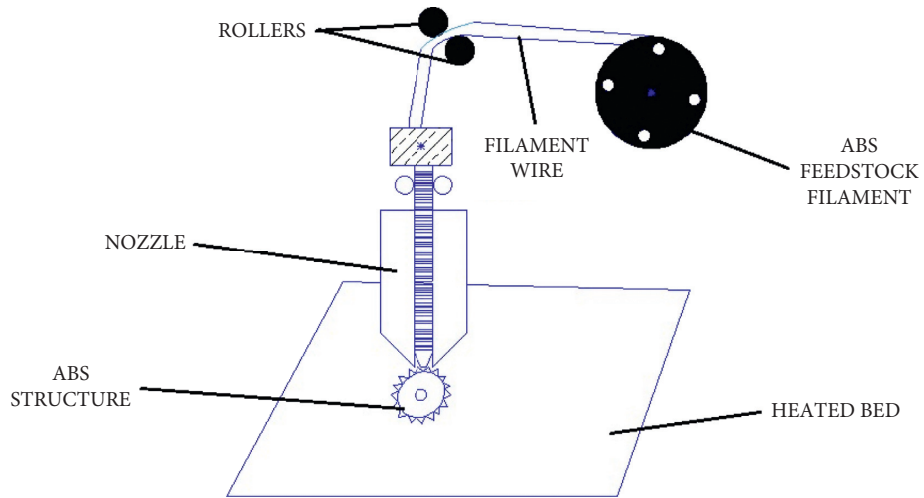


FIGURE 1: Schematic diagram of layer-by-layer deposition of ABS material.

TABLE 1: Process parameters and their levels.

Exp no.	Infill pattern	Nozzle temperature (°C)	Printing speed (mm/s)
1	Lines	210	60
2	Lines	230	70
3	Lines	250	80
4	Triangles	210	70
5	Triangles	230	80
6	Triangles	250	60
7	Tetrahedral	210	80
8	Tetrahedral	230	60
9	Tetrahedral	250	70



FIGURE 2: Image of 3D-printed parts.

TABLE 2: Readings of surface roughness tester.

Exp. no.	Reading no. 1	Reading no. 2	Reading no. 3	Mean value
1	1.99	2.48	2.43	2.30
2	1.52	1.44	1.81	1.59
3	2.29	2.39	2.43	2.37
4	1.14	1.03	0.95	1.50
5	2.85	2.40	2.67	2.64
6	1.97	2.51	2.32	2.26
7	1.54	1.71	1.82	1.69
8	1.99	2.35	2.23	2.19
9	1.80	1.48	1.41	1.56

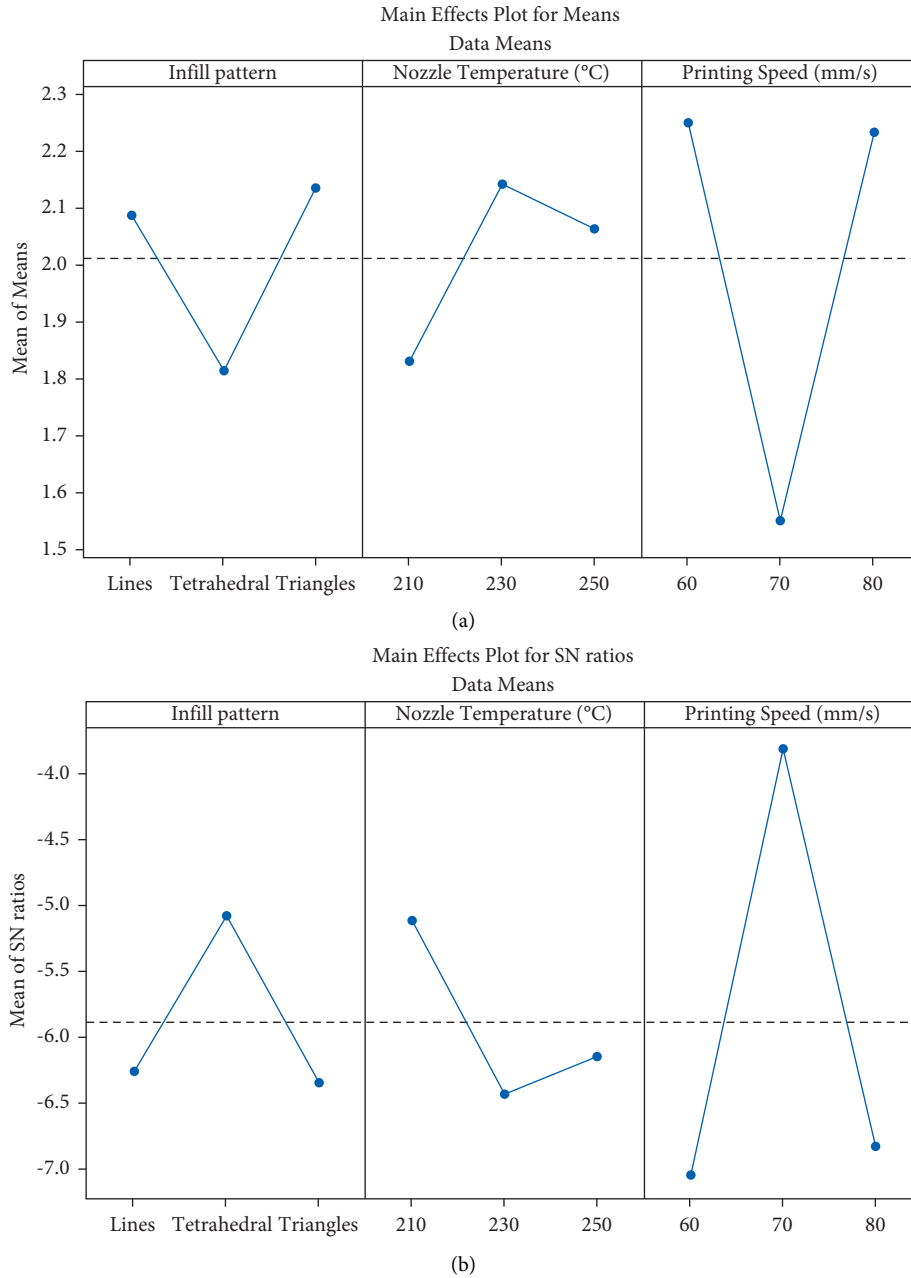


FIGURE 3: Effect of variable parameters on surface roughness: (a) mean values and (b) SN ratio.

TABLE 3: ANOVA test results for surface roughness.

Source	DF	Seq. SS	Adj. SS	Seq. MS	P value	F value	Percentage contribution (%)
Infill pattern	2	0.12449	0.12449	0.06225	0.371	1.70	4.76
Nozzle temperature	2	0.23650	0.23650	0.11825	0.237	3.23	9.04
Printing speed	2	2.18278	2.18278	1.09139	0.032	29.78	83.41
Error	2	0.07330	0.07330	0.03665			2.80
Total	8	2.61707					100.00

5. Multiobjective Optimization of Process Parameters Using Genetic Algorithm

The regression method is applied to investigate the effect of input on output. SPSS software is used to apply the

regression method. The present work is focused on three response parameters; therefore, three single-objective equations are formulated with the help of the regression method. To optimize the process parameters, the mathematical model must be formulated which is further used as

TABLE 4: Reading of thickness measurement.

Exp. no.	Reading no. 1	Reading no. 2	Reading no. 3	Mean value
1	6.20	6.22	6.22	6.21
2	6.20	6.24	6.26	6.23
3	6.24	6.26	6.28	6.26
4	6.16	6.20	6.24	6.20
5	6.20	6.22	6.22	6.21
6	6.18	6.20	6.22	6.20
7	6.24	6.26	6.24	6.24
8	6.20	6.22	6.22	6.20
9	6.20	6.24	6.26	6.23

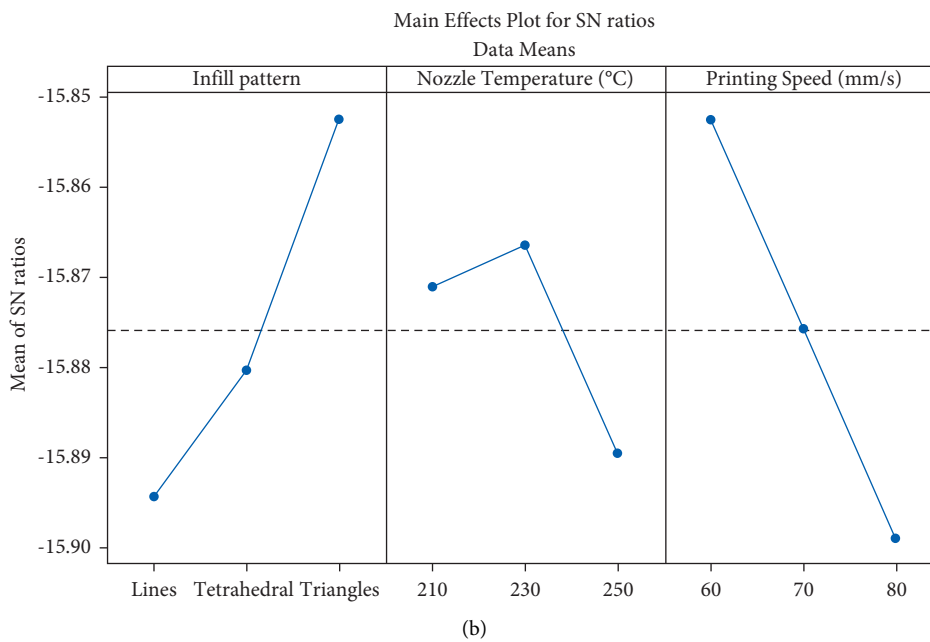
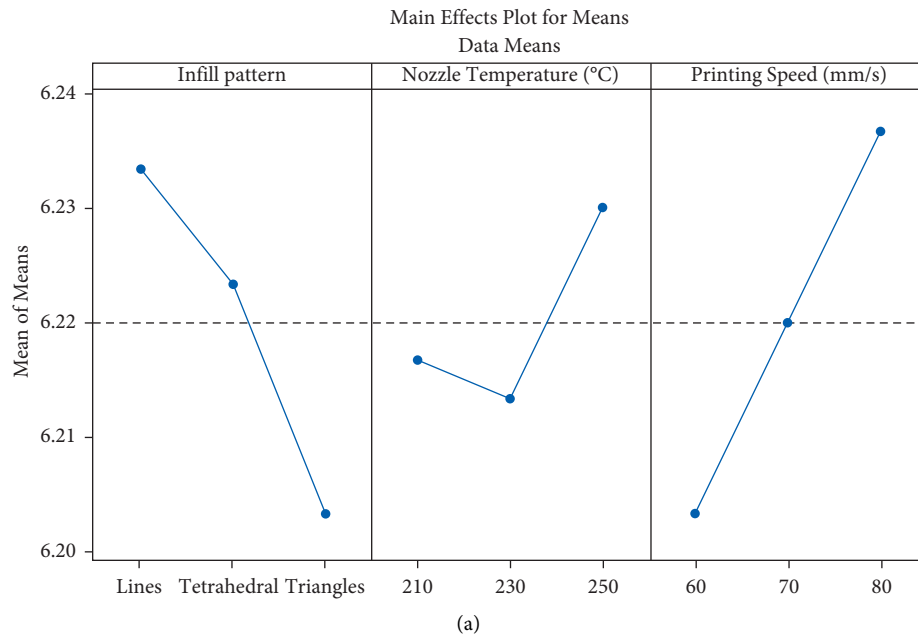


FIGURE 4: Effect of variable parameters on the thickness: (a) mean values and (b) SN ratio.

TABLE 5: ANOVA test results for thickness.

Source	DF	Seq. SS	Adj. SS	Seq. MS	P value	F value	Percentage contribution (%)
Infill pattern	2	0.001389	0.001389	0.000694	0.045	21.39	39.07
Nozzle temperature	2	0.000453	0.000453	0.000227	0.125	6.99	12.76
Printing speed	2	0.001648	0.001648	0.000824	0.125	25.39	46.35
Error	2	0.000065	0.000065	0.000032			1.83
Total	8	0.003555					100.00

TABLE 6: Measurements of outer diameter.

Exp. no.	Reading no. 1	Reading no. 2	Reading no. 3	Mean value
1	32.70	32.74	32.72	32.72
2	32.56	32.60	32.64	32.60
3	32.60	32.64	32.62	32.62
4	32.58	32.60	32.62	32.60
5	32.64	32.64	32.64	32.64
6	32.68	32.72	32.70	32.70
7	32.54	323.70	32.66	32.60
8	32.66	32.70	32.68	32.68
9	32.60	32.60	32.60	32.60

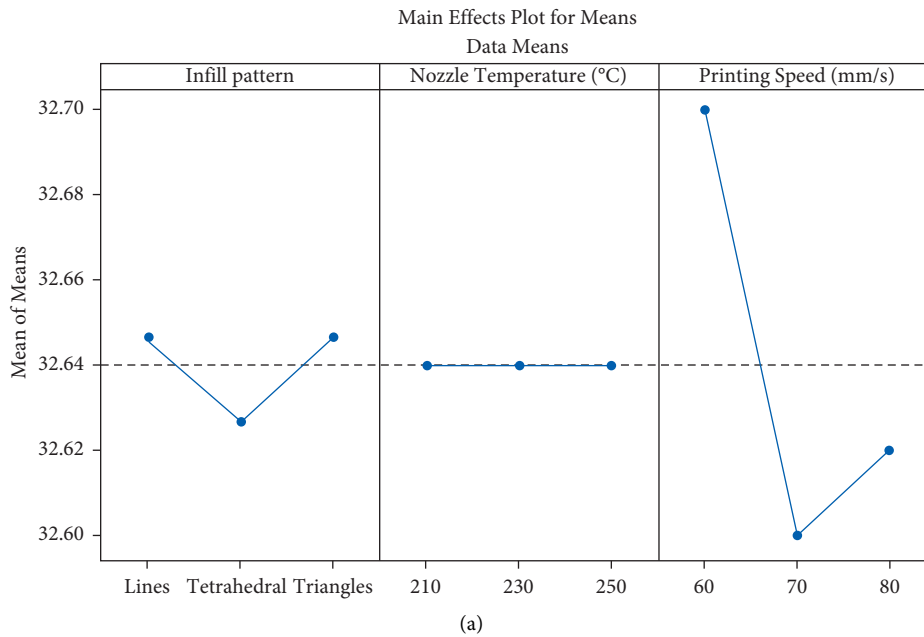


FIGURE 5: Continued.

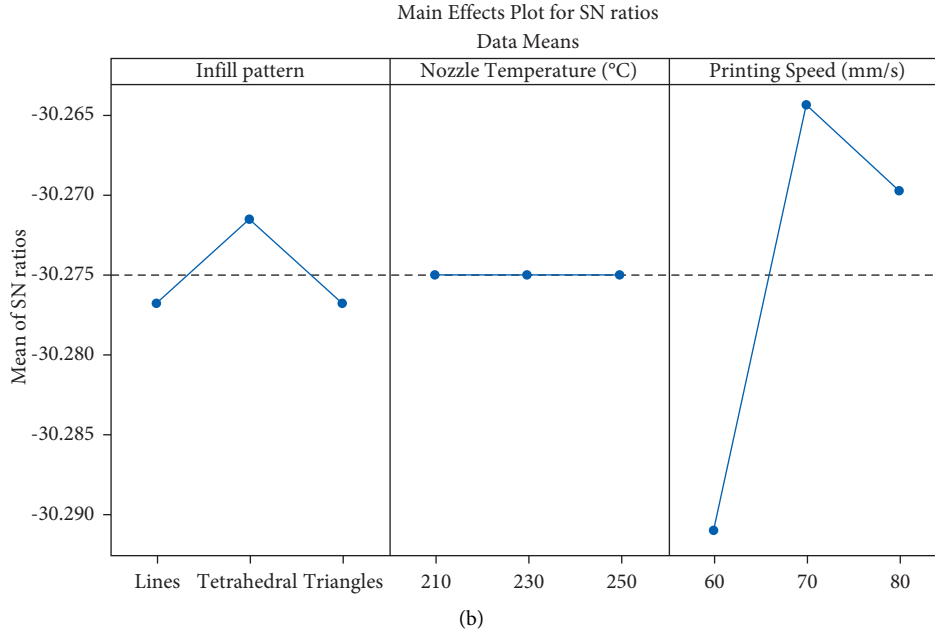


FIGURE 5: Effect of variable parameters on the outer diameter: (a) mean values and (b) SN ratio.

TABLE 7: ANOVA test results for diameter.

Source	DF	Seq. SS	Adj. SS	Seq. MS	<i>P</i> value	<i>F</i> value	Percentage contribution (%)
Infill pattern	2	0.0000	0.0000	0.0000	0.99	0.503	0.58
Nozzle temperature	2	0.0000	0.0000	0.0000	19.05	0.050	11.22
Printing speed	2	0.0000	0.0000	0.0000	148.72	0.007	87.61
Error	2	0.0000	0.0000	0.0000			0.59
Total	8	0.0000					100.00

an objective function for optimization. The mathematical model defines a relationship between input and output parameters. In the present context, there are three main process variables of the FDM process, whereas SR, T_c , and

D_c are output parameters. Three equations are developed, one for each output, using regression methods, where minimization of SR, T_c , and D_c are the objectives' function:

$$\begin{aligned}
 SR_{\text{MIN}} &= 32.33 - 1.870A + 0.09217B - 1.142C - 0.1833A * A - 0.000267B * B \\
 &\quad + 0.008517C * C + 0.01600A * B - 0.01733A * C, \\
 TC_{\text{MIN}} &= 0.9529 - 0.05167A - 0.008500B + 0.005333C + 0.02500A * A \\
 &\quad + 0.000021B * B - 0.000033C * C - 0.000333A * B + 0.000333A * C, \\
 DC_{\text{MIN}} &= -5.935 + 0.7200A + 0.02800B + 0.07100C - 0.01000A * A - 0.000050B * B \\
 &\quad - 0.000500C * C - 0.003000A * B - 0.000000A * C.
 \end{aligned} \tag{1}$$

Genetic algorithm is a nature-based algorithm used to solve nonlinear objective functions. Holland (1960) developed the GA and further modified it by Goldberg in 1989. GA is used to achieve the best fitness values and its results are more reliable, especially in a constrained optimization problem, as shown in Figure 6.

The result of GA showed that the infill pattern should be at higher values for minimizing the surface roughness, change in diameter, and multiobjective optimization [36–69]. The value

of the infill pattern should be 2, if we are considering minimizing the change in thickness only. The notable finding of this work is the printing speed should not be at the highest level as suggested by all single objectives and multiobjective function values. The value of the printing speed should be at a minimum, i.e., 60 for minimizing the change in thickness and diameter. The value of the printing speed should be 70 for minimizing the surface roughness and also suggested by multiobjective optimization. The value of

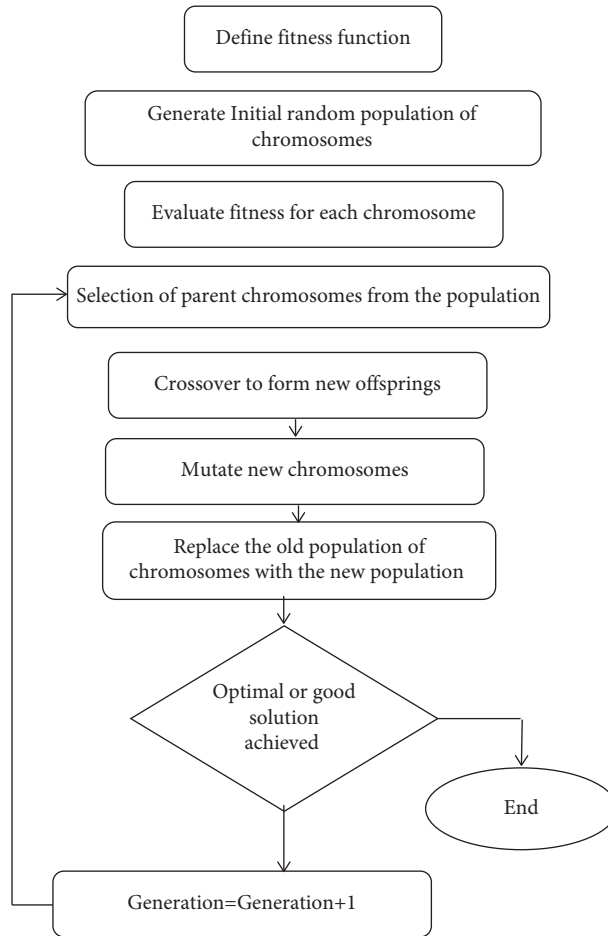


FIGURE 6: Flow diagram of GA.

TABLE 8: Output of genetic algorithm.

Optimization	Objective function value	Infill pattern	Nozzle temperature	Printing speed
SR _{MIN}	0.885	3.000	210.000	70.094
TC _{MIN}	0.190	2.092	218.965	60.000
DC _{MIN}	0.220	3.000	250.000	60.000
Multiobjective	0.520	3.000	210.000	69.931

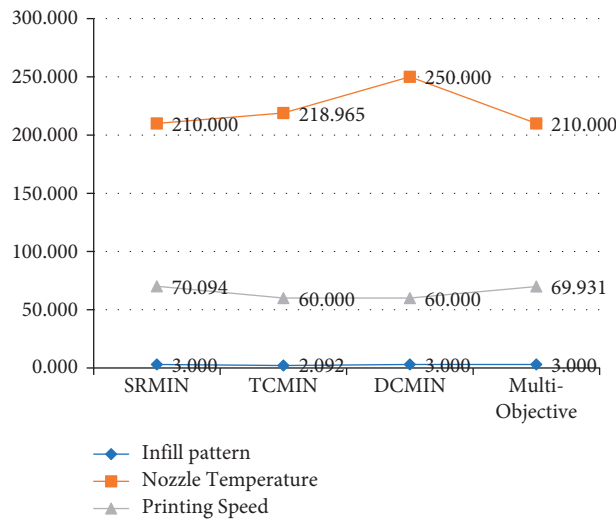


FIGURE 7: Values of process parameters for optimization.

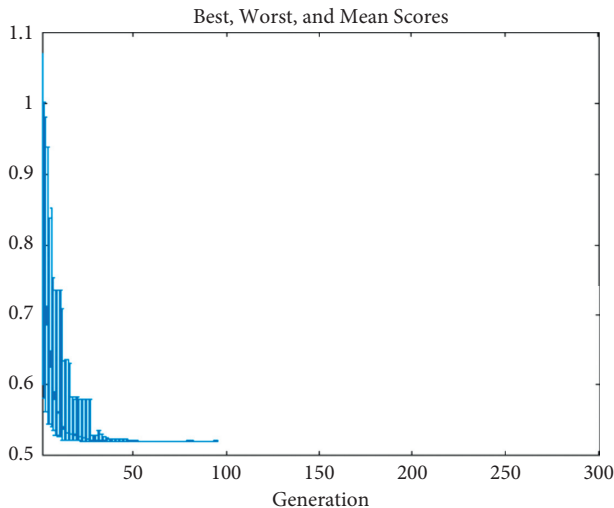


FIGURE 8: The number of iterations in multiobjective function.

nozzle temperature should be 210 for minimizing the surface roughness and also suggested by multiobjective function results. The results of GA are presented in Table 8 and Figure 7. Figure 8 represents the number of iterations and objective function value. The minimum objective values achieved 0.520 in multiobjective optimization.

6. Conclusions

In the present research, 3D printing of gear-shaped specimens made up of ABS is carried out and the effect of an infill shape pattern, built plate temperature, and nozzle speed on surface finish and thickness is investigated. The most influencing factor is printing speed. The results obtained can be summarized as follows:

- (i) Surface finish in ABS depends on nozzle speed; low nozzle speed tends to better surface finish. The effect of changing the printing speed is very much satisfying.
- (ii) In the aspect of thickness measurement, all the readings are almost the same and there is a little variation from the actual design due to the gum applied on the bed but this is almost constant in each part.
- (iii) Measurement of the outer diameter also gives the almost constant reading in each part, and observed reading is less than the actual drawing value.
- (iv) Results of GA suggested that the value of infill pattern and nozzle temperature should be at level 1, and the value of printing speed should be at level 2 for achieving optimized results.

In the present examination, the impacts of parameters like shape pattern design, built plate temperature, and nozzle speed were examined for surface finish and thickness. In future, the impact of different parameters, for example, orientation and layer height, can be researched. The impact of these parameters on some other printing materials like

PLA and so forth can likewise be explored. The impact of these parameters on composite 3D-printed structures can likewise be examined. FDM printer design can be improved for better accuracy of surface finish and dimensions.

Data Availability

The data used to support the findings of this study are included within the article.

Conflicts of Interest

The authors declare that there are no conflicts of interest.

References

- [1] Z. Chen, Z. Li, J. Li et al., "3D printing of ceramics: a review," *Journal of the European Ceramic Society*, vol. 39, no. 4, pp. 661–687, 2019.
- [2] Y. Gao, Y. Zhao, G. Zhang, F. Yin, and H. Zhang, "Modeling of material removal in magnetic abrasive finishing process with spherical magnetic abrasive powder," *International Journal of Mechanical Sciences*, vol. 177, Article ID 105601, 2020.
- [3] L. C. P. Dos Santos, F. C. Malheiros, and A. Z. Guarato, "Surface parameters of as-built additive manufactured metal for intraosseous dental implants," *The Journal of Prosthetic Dentistry*, vol. 124, no. 2, pp. 217–222, 2020.
- [4] A. Sedmak, K. Čolić, A. Grbović, I. Balać, and M. Burzić, "Numerical analysis of fatigue crack growth of hip implant," *Engineering Fracture Mechanics*, vol. 216, Article ID 106492, 2019.
- [5] H. Liu, H. Liu, C. Zhu, and J. Tang, "Study on gear contact fatigue failure competition mechanism considering tooth wear evolution," *Tribology International*, Article ID 106277, 2020.
- [6] J. Li, C. Wu, P. K. Chu, and M. Gelinsky, "3D printing of hydrogels: rational design strategies and emerging biomedical applications," *Materials Science and Engineering: R: Reports*, vol. 140, Article ID 100543, 2020.
- [7] L. E. Murr, "Frontiers of 3D printing/additive manufacturing: from human organs to aircraft fabrication†," *Journal of Materials Science & Technology*, vol. 32, no. 10, pp. 987–995, 2016.
- [8] A. K. Matta, S. Prasad Kodali, J. Ivvala, and P. J. Kumar, "Metal prototyping the future of automobile industry: a review," *Materials Today Proceedings*, vol. 5, no. 9, Article ID 17597, 2018.
- [9] R. Kumar and R. Kumar, "3D printing of food materials: a state of art review and future applications," *Materials Today Proceedings*, vol. 33, pp. 1463–1467, 2020.
- [10] T.-C. Huang and C.-Y. Lin, "From 3D modeling to 3D printing: development of a differentiated spatial ability teaching model," *Telematics and Informatics*, vol. 34, no. 2, pp. 604–613, 2017.
- [11] W. S. W. Harun, N. S. Manam, M. S. I. N. Kamariah et al., "A review of powdered additive manufacturing techniques for Ti-6Al-4V biomedical applications," *Powder Technology*, vol. 331, pp. 74–97, 2018.
- [12] F. P. W. Melchels, J. Feijen, and D. W. Grijpma, "A review on stereolithography and its applications in biomedical engineering," *Biomaterials*, vol. 31, no. 24, pp. 6121–6130, 2010.

- [13] E. O. Olakanmi, R. F. Cochrane, and K. W. Dalgarno, "A review on selective laser sintering/melting (SLS/SLM) of aluminium alloy powders: processing, microstructure, and properties," *Progress in Materials Science*, vol. 74, pp. 401–477, 2015.
- [14] L. Yuan, S. Ding, and C. Wen, "Additive manufacturing technology for porous metal implant applications and triple minimal surface structures: a review," *Bioactive Materials*, vol. 4, pp. 56–70, 2019.
- [15] D. Singh, R. Singh, and K. S. Boparai, "Development and surface improvement of FDM pattern based investment casting of biomedical implants: a state of art review," *Journal of Manufacturing Processes*, vol. 31, pp. 80–95, 2018.
- [16] S. Garzon-Hernandez, D. Garcia-Gonzalez, A. Jérusalem, and A. Arias, "Design of FDM 3D printed polymers: an experimental-modelling methodology for the prediction of mechanical properties," *Materials & Design*, vol. 188, Article ID 108414, 2020.
- [17] J. Oliveira, V. Correia, H. Castro, P. Martins, and S. Lanceros-Mendez, "Polymer-based smart materials by printing technologies: improving application and integration," *Additive Manufacturing*, vol. 21, pp. 269–283, 2018.
- [18] D. G. Bekas, Y. Hou, Y. Liu, and A. Panesar, "3D printing to enable multifunctionality in polymer-based composites: a review," *Composites Part B: Engineering*, vol. 179, Article ID 107540, 2019.
- [19] W. Zhu, X. Ma, M. Gou, D. Mei, K. Zhang, and S. Chen, "3D printing of functional biomaterials for tissue engineering," *Current Opinion in Biotechnology*, vol. 40, pp. 103–112, 2016.
- [20] K. Markstedt, K. Håkansson, G. Toriz, and P. Gatenholm, "Materials from trees assembled by 3D printing - wood tissue beyond nature limits," *Applied Materials Today*, vol. 15, pp. 280–285, 2019.
- [21] G. Zhang, D. Carloni, and Y. Wu, "3D printing of transparent YAG ceramics using copolymer-assisted slurry," *Ceramics International*, vol. 46, 2020.
- [22] S. C. Daminabo, S. Goel, S. A. Grammatikos, H. Y. Nezhad, and V. K. Thakur, "Fused deposition modeling-based additive manufacturing (3D printing): techniques for polymer material systems," *Materials Today Chemistry*, vol. 16, Article ID 100248, 2020.
- [23] F. Ali and B. V. Chowdary, "Natural Frequency prediction of FDM manufactured parts using ANN approach," *IFAC-PapersOnLine*, vol. 52, no. 13, pp. 403–408, 2019.
- [24] V. Wankhede, D. Jagetiya, A. Joshi, and R. Chaudhari, "Experimental investigation of FDM process parameters using Taguchi analysis," *Materials Today Proceedings*, vol. 27, no. 3, pp. 2117–2120, 2020.
- [25] J. S. Chohan, R. Singh, and K. S. Boparai, "Mathematical modelling of surface roughness for vapour processing of ABS parts fabricated with fused deposition modelling," *Journal of Manufacturing Processes*, vol. 24, pp. 161–169, 2016.
- [26] P. Wang, B. Zou, and S. Ding, "Modeling of surface roughness based on heat transfer considering diffusion among deposition filaments for FDM 3D printing heat-resistant resin," *Applied Thermal Engineering*, vol. 161, Article ID 114064, 2019.
- [27] T. Peng and F. Yan, "Dual-objective analysis for desktop FDM printers: energy consumption and surface roughness," *Procedia CIRP*, vol. 69, pp. 106–111, 2018.
- [28] D. Yadav, D. Chhabra, R. K. Gupta, A. Phogat, and A. Ahlawat, "Modeling and analysis of significant process parameters of FDM 3D printer using ANFIS," *Materials Today Proceedings*, vol. 21, pp. 1592–1604, 2020.
- [29] M. S. Khan, S. B. Mishra, M. A. Kumar, and D. Banerjee, "Optimizing surface texture and coating thickness of nickel coated ABS-3D parts," *Materials Today Proceedings*, vol. 5, no. 9, Article ID 19011, 2018.
- [30] N. Sajan, T. D. John, M. Sivadasan, and N. K. Singh, "An investigation on circularity error of components processed on Fused Deposition Modeling (FDM)," *Materials Today Proceedings*, vol. 5, no. 1, pp. 1327–1334, 2018.
- [31] M. Ehsanul Haque, D. Banerjee, S. Bikash Mishra, and B. Kumar Nanda, "A numerical approach to measure the surface roughness of FDM build part," *Materials Today Proceedings*, vol. 18, pp. 5523–5529, 2019.
- [32] I. Farina, R. Goodall, E. Hernández-Nava, A. di Filippo, F. Colangelo, and F. Fraternali, "Design, microstructure and mechanical characterization of Ti6Al4V reinforcing elements for cement composites with fractal architecture," *Materials & Design*, vol. 172, Article ID 107758, 2019.
- [33] K. Hibbert, G. Warner, C. Brown, O. Ajide, G. Owolabi, and A. Azimi, "The effects of build parameters and strain rate on the mechanical properties of FDM 3D-Printed acrylonitrile Butadiene Styrene," *Open Journal of Organic Polymer Materials*, vol. 09, no. 01, pp. 1–27, 2019.
- [34] H. Dou, W. Ye, D. Zhang, Y. Cheng, and Y. Tian, "Compression performance with different build orientation of fused filament fabrication polylactic acid, acrylonitrile butadiene styrene, and polyether ether ketone," *Journal of Materials Engineering and Performance*, pp. 1–9, 2021.
- [35] Y. Wang, X. Li, Y. Chen, and C. Zhang, "Strain rate dependent mechanical properties of 3D printed polymer materials using the DLP technique," *Additive Manufacturing*, vol. 47, Article ID 102368, 2021.
- [36] R. A. Ilyas, S. M. Sapuan, M. R. M. Asyraf et al., "Polymer composites filled with metal derivatives: a review of flame retardants," *Polymers*, vol. 13, no. 11, p. 1701, 2021.
- [37] S. Prabhakaran, V. Krishnaraj, S. Sharma, M. Senthilkumar, R. Jegathishkumar, and R. Zitoune, "Experimental study on thermal and morphological analyses of green composite sandwich made of flax and agglomerated cork," *Journal of Thermal Analysis and Calorimetry*, vol. 139, no. 5, pp. 3003–3012, 2020.
- [38] S. Sharma, P. Sudhakara, J. Singh, R. A. Ilyas, M. R. M. Asyraf, and M. R. Razman, "Critical review of biodegradable and bioactive polymer composites for bone tissue engineering and drug delivery applications," *Polymers*, vol. 13, no. 16, p. 2623, 2021.
- [39] S. Sharma, P. Sudhakara, A. A. B. Omran, J. Singh, and R. A. Ilyas, "Recent trends and developments in conducting polymer nanocomposites for multifunctional applications," *Polymers*, vol. 13, no. 17, p. 2898, 2021.
- [40] K. Jha, Y. K. Tyagi, R. Kumar et al., "Assessment of dimensional stability, biodegradability, and fracture energy of bio-composites reinforced with novel pine cone," *Polymers*, vol. 13, no. 19, p. 3260, 2021.
- [41] A. Kadier, R. A. Ilyas, M. R. M. Huzaiifah et al., "Use of industrial wastes as sustainable nutrient sources for bacterial cellulose (BC) production: mechanism, advances, and future perspectives," *Polymers*, vol. 13, no. 19, p. 3365, 2021.
- [42] Y. Singh, J. Singh, S. Sharma, T.-D. Lam, and D.-N. Nguyen, "Fabrication and characterization of coir/carbon-fiber reinforced epoxy based hybrid composite for helmet shells and sports-good applications: influence of fiber surface modifications on the mechanical, thermal and morphological properties," *Journal of Materials Research and Technology*, vol. 9, no. 6, Article ID 15593, 2020.

- [43] M. J. Suriani, R. A. Ilyas, M. Y. M. Zuhri et al., "Critical review of natural fiber reinforced hybrid composites: processing, properties, applications and cost," *Polymers*, vol. 13, no. 20, p. 3514, 2021.
- [44] R. Kumar, N. Ranjan, V. Kumar et al., "Characterization of friction stir-welded polylactic acid/aluminum composite primed through fused filament fabrication," *Journal of Materials Engineering and Performance*, 2021.
- [45] R. A. Ilyas, M. Y. M. Zuhri, M. N. F. Norrrahim et al., "Natural fiber-reinforced polycaprolactone green and hybrid bio-composites for various advanced applications," *Polymers*, vol. 14, no. 1, p. 182, 2022.
- [46] M. N. M. Azlin, R. A. Ilyas, M. Y. M. Zuhri et al., "3D printing and shaping polymers, composites, and nanocomposites: a review," *Polymers*, vol. 14, no. 1, p. 180, 2022.
- [47] J. Kumar, D. Singh, N. S. Kalsi et al., "Comparative study on the mechanical, tribological, morphological and structural properties of vortex casting processed, Al-SiC-Cr hybrid metal matrix composites for high strength wear-resistant applications: fabrication and characterizations," *Journal of Materials Research and Technology*, vol. 9, no. 6, Article ID 13607, 2020.
- [48] S. P. Dwivedi, A. Saxena, and S. Sharma, "Influence of nano-CuO on synthesis and mechanical behavior of spent alumina catalyst and grinding sludge reinforced aluminum based composite," *International Journal of Metalcasting*, vol. 16, 2021.
- [49] R. N. Muni, J. Singh, V. Kumar, and S. Sharma, "Parametric optimization of rice husk ash, copper, magnesium reinforced aluminium matrix hybrid composite processed by EDM," *ARPN Journal of Engineering and Applied Sciences*, vol. 14, no. 22, 2019.
- [50] R. N. Muni, J. Singh, V. Kumar, and S. Sharma, "Influence of rice husk ash, Cu, Mg on the mechanical behaviour of Aluminium Matrix hybrid composites," *International Journal of Applied Engineering Research*, vol. 14, no. 8, pp. 1828–1834.
- [51] S. P. Dwivedi, A. Saxena, S. Sharma, A. K. Srivastava, and N. K. Maurya, "Influence of SAC and eggshell addition in the physical, mechanical and thermal behaviour of Cr reinforced aluminium based composite," *International Journal of Cast Metals Research*, vol. 34, no. 1, pp. 43–55.
- [52] A. Saxena, S. P. Dwivedi, A. Dixit, S. Sharma, A. K. Srivastava, and N. K. Maurya, "Computational and experimental investigation on mechanical behavior of zirconia toughened alumina and nickel powder reinforced EN31 based composite material," *Materialwissenschaft und Werkstofftechnik*, vol. 52, no. 5, pp. 548–560, 2021.
- [53] S. Sharma, J. Singh, M. K. Gupta et al., "Investigation on mechanical, tribological and microstructural properties of Al-Mg-Si-T6/SiC/muscovite-hybrid metal-matrix composites for high strength applications," *Journal of Materials Research and Technology*, vol. 12, no. 21, pp. 1564–1581, 2021.
- [54] S. P. Dwivedi, R. Agrawal, and S. Sharma, "Effect of friction stir process parameters on mechanical properties of chrome containing leather waste reinforced aluminium based composite," *International Journal of Precision Engineering and Manufacturing-Green Technology*, vol. 8, no. 3, pp. 935–943, 2021.
- [55] J. Kumar, D. Singh, N. S. Kalsi et al., "Investigation on the mechanical, tribological, morphological and machinability behavior of stir-casted Al/SiC/Mo reinforced MMCs," *Journal of Materials Research and Technology*, vol. 12, pp. 930–946, 2021.
- [56] V. Aggarwal, J. Singh, S. Sharma, A. Sharma, G. Singh, and J. Parshad, "Empirical modeling of machining parameters during WEDM of inconel 690 using response surface methodology," *AIP Conference Proceedings*, vol. 2281, Article ID 020032, 2020.
- [57] V. Aggarwal, J. Singh, S. Sharma, K. Harish, A. Garg, and G. Sharma, "An experimental study of wire breakage frequency on different electrodes during WEDM of Inconel-722," *IOP Conference Series: Materials Science and Engineering*, vol. 954, Article ID 12013, 2020.
- [58] V. Aggarwal, C. I. Pruncu, J. Singh, S. Sharma, and D. Y. Pimenov, "Empirical investigations during WEDM of Ni-27Cu-3.15Al-2Fe-1.5Mn based superalloy for high temperature corrosion resistance applications," *Materials*, vol. 13, no. 16, p. 3470, 2020.
- [59] M. R. Qureshi, S. Sharma, J. Singh, S. A. Khadar, and R. U. Baig, "Evaluation of surface roughness in the turning of mild steel under different cutting conditions using back-propagation neural network," *Proceedings of the Estonian Academy of Sciences*, vol. 69, no. 2, pp. 109–115, 2020.
- [60] S. Islam, S. P. Dwivedi, V. K. Dwivedi, S. Sharma, and D. Kozak, "Development of marble dust/waste PET based polymer composite material for environmental sustainability: fabrication and characterizations," *Journal of Materials Performance and Characterization*, vol. 10, no. 1, pp. 538–552, 2021.
- [61] S. Sharma and P. Sudhakara, "Fabrication and optimization of hybrid AA-6082-T6 alloy/8%Al₂O₃(Alumina)/2%Grp metal matrix composites using novel Box-Behnken methodology processed by wire-sinking electric discharge machining," *Materials Research Express*, vol. 6, no. 11, 2019.
- [62] H. Singh, J. Singh, S. Sharma, S. P. Dwivedi, and A. J. Obaid, "Comparative performance of copper, graphite, brass and aluminium/graphite based different tool electrodes for optimizing the material removal rate during die-sinking EDM of stir-casted, Al6061/SiC MMCs for sustainable manufacturing and energy applications," *Journal of Green Engineering*, vol. 11, no. 1, pp. 922–938, 2021.
- [63] S. P. Dwivedi, A. Saxena, S. Sharma et al., "Effect of ball-milling process parameters on mechanical properties of Al/Al₂O₃/collagen powder composite using statistical approach," *Journal of Materials Research and Technology*, vol. 15, pp. 2918–2932, 2021.
- [64] J. M. Khare, S. Dahiya, B. Gangil et al., "Comparative analysis of erosive wear behaviour of epoxy, polyester and vinyl esters based thermosetting polymer composites for human prosthetic applications using Taguchi design," *Polymers*, vol. 13, no. 20, p. 3607, 2021.
- [65] S. P. Dwivedi, N. Maurya, and S. Sharma, "Study of CCLW, alumina and the mixture of alumina and CCLW reinforced aluminum based composite material with and without mechanical alloying," *Journal of the Institution of Engineers (India): Series D*, 2021.
- [66] S. P. Dwivedi, R. Sahu, A. Saxena, V. K. Dwivedi, K. Srinivas, and S. Sharma, "Recovery of Cr from chrome-containing leather waste and its utilization as reinforcement along with waste spent alumina catalyst and grinding sludge in AA 5052-based metal matrix composites," *Part E: Journal of Process Mechanical Engineering*, 2021.
- [67] S. P. Dwivedi, M. Maurya, A. Saxena, and S. Sharma, "Synthesis and characterization of spent alumina catalyst and grinding sludge reinforced aluminium-based composite material," *Proceedings of the Institution of Mechanical*

Engineers - Part C: Journal of Mechanical Engineering Science.
12 pages, 2021.

- [68] S. P. Dwivedi and S. Sharma, "Synthesis and Characterization of Cr, Eggshell and Grinding Sludge Reinforced Aluminum Based Metal Matrix Composites: An Ingenious Experimental Approach," *Green Materials (ICE Virtual)*, 2021.